# Polymer Chemistry

www.rsc.org/polymers

# Supramolecular polymer networks based on cucurbit[8]uril host−guest interactions as aqueous photo-rheological fluids†

Cindy S. Y. Tan,[a,b] Jesús del Barrio,*[a,c] Ji Liu[a] and Oren A. Scherman*[a]

We describe a low-mass fraction (≤0.75 wt%) supramolecular polymer network as an aqueous photo-rheological fluid (PRF) whose rheological properties can be easily modulated *via* light irradiation. This supramolecular polymer network is formed *via* CB[8]-assisted host−guest interactions between naphthyl-functionalised hydroxyethyl cellulose (HEC-Np), methyl viologen containing styrene copolymer (PSTMV), cucurbit[8]uril (CB[8]) and a photoisomerisable azobenzene imidazolium (AzoIm) derivative. This cellulose-based PRF can undergo a UV-triggered rapid transition from a highly viscous and rigid gel into a Newtonian-like fluid, with a decrease in zero-shear viscosity of over two orders of magnitude. Moreover, the rate of viscosity reduction of these PRFs can be tuned based on the mixture composition and duration of photoirradiation.

## 1. Introduction

Smart rheological fluids are fluids whose rheological behaviour can be modulated by applying a stimulus, such as temperature, pH, light, magnetic and electric fields.[1] The ability to rapidly and reversibly change the rheological properties of these smart fluids, upon application of an external stimulus, has made them attractive for intelligent devices, such as valves, haptic controllers, tactile displays, clutches and shock absorbers of vehicles and buildings.[2–4] Based on the origin of the stimulus, these smart fluids can be classified as magneto-rheological fluids (MRFs), electro-rheological fluids (ERFs) and photo-rheological fluids (PRFs). MRFs and ERFs are comprised of micro- or nanoparticles suspended in a dielectric carrier liquid. In most cases, these fluids are abrasive in nature and potentially suffer from the aggregation of a heterogeneous

colloidal suspension with time.[3,5,6] Such drawbacks make PRFs more attractive for their homogeneous nature that allows photomodulation of their properties on a nanoscale.[5] Compared to other stimuli, light is desirable because it does not contaminate the reaction system and can be delivered remotely and instantly with high accuracy.[7,8] Moreover, the light resolution and activation can be controlled precisely by the photon intensity and/or wavelength.[9]

A variety of PRFs have been developed so far, but they have mostly relied on noncovalent interactions including hydrogen bonding, hydrophobic interactions, electrostatic effects and van der Waals forces. In principle, the mechanism of fine-tuning of the rheological properties lies in the reversible conformation transition of the light-sensitive moieties. Therefore, the photo-induced molecular rearrangement within the fluid affects the macroscopic viscosity of the material. Raghavan and coworkers have demonstrated PRFs based on simple and commercially available small molecules, such as *trans-ortho*-methoxycinnamic acid (OMCA) and coumarin derivatives. Taking the OMCA-system as an example, photo-induced isomerisation of *trans*-OMCA to *cis*-OMCA decreased the size of micelles, thus the reduced intermicellar interactions resulted in a thin fluid. Viscosities of PRFs change dramatically with UV irradiation to obtain photothinning[5,10–12] and photogelling effects.[10,13,14] Moreover, to the best of our knowledge, all previous examples of PRFs fabricated by direct formation mechanisms have been reported to contain higher than a 2 wt% mass fraction of materials, such as a 7 wt% LAPONITE® colloidal dispersion.[13] Such a high content of chromophores, above a threshold concentration, might be problematic for

*[a]Melville Laboratory for Polymer Synthesis, Department of Chemistry, University of Cambridge, Cambridge, CB2 1EW, UK. E-mail: oas23@cam.ac.uk; Fax: +44 (0)1223 334866; Tel: +44 (0)1223 331508*
*[b]Faculty of Applied Sciences, Universiti Teknologi MARA, Kampus Kota Samarahan, Jalan Meranek, 94300 Kota Samarahan, Sarawak, Malaysia*
*[c]Gould Research Center, Schlumberger, High Cross, Madingley Road, Cambridge CB3 0EL, UK. E-mail: JBarrio2@slb.com*

†Electronic supplementary information (ESI) available: Experimental details, ITC curves and ^{1}H NMR spectra of complexation/decomplexation of model compounds with CB[8], rheological measurements of control samples using AzoTEG, self-healing properties of the HEC-based network, concentration- and irradiation period-dependent studies on photo-induced viscosity change, *etc.* CCDC 1413215. For ESI and crystallographic data in CIF or other electronic format see DOI: 10.1039/c5py01115a

certain applications, where strong absorption of the chromophores is undesirable.[15]

We have previously described that polymers functionalised with first and second guest molecules, typically viologen and naphthyl derivatives, respectively, can self-assemble to form dynamically crosslinked networks in the presence of cucurbit-[8]uril (CB[8]).[16,17] Certain photoswitchable molecules have shown a photocontrolled binding affinity for CB[8], where some cationic azobenzene derivatives demonstrate stronger binding association with CB[8] in their *cis* conformations.[18,19] We envisioned that by incorporating a small photochromic molecule with a phototunable binding affinity as a competing guest, it would be possible to transform a non-responsive dynamic gel into a light-sensitive system. Our approach to PRFs employs naphthyl-functionalised hydroxyethyl cellulose (HEC-Np, **P5**), viologen-bearing polymer (PSTMV, **P4**), competitive chromophore 1-[*p*-(phenylazo)benzyl)]imidazolium (AzoIm, *E*-**3**) and CB[8] as the macrocyclic host molecules (Fig. 1). This strategy involves starting materials that are readily available,

facile fabrication steps and extremely low solid contents, making our system more promising as a PRF.

## 2. Results and discussion

### 2.1 Complexation–decomplexation mechanism of CB[8] and guests

^{1}H NMR spectroscopy was first used to demonstrate the host–guest complexation between CB[8] and the guests in aqueous solution (ESI, Fig. S1 and S2†). We selected doubly-charged methyl viologen (MV$^{2+}$, **1**) and 5000 Da polyethylene glycol monofunctionalised with a naphthyl (PEG-Np, **2**) as the model molecules (Fig. 1a). AzoIm (*E*-**3**) was then introduced as the competitive second guest to investigate the photoresponsive properties of the system (Fig. 1b) because of its aqueous solubility and its *cis* isomer shows a higher binding affinity to CB[8] than those of neutral azobenzene derivatives. The appearance of new broad peaks downfield upon addition of *E*-**3** suggests the formation of CB[8]·**1**·*E*-**3**. At equilibrium, CB[8]·**1**·**2** and CB[8]·**1**·*E*-**3** complexes coexist in the solution (ESI, Fig. S2e†). The CB[8]·**1**·**2** complex is likely the predominant species on account of the higher binding affinity of **2** to CB[8]·**1** over that of the azobenzene species ($K_{Np} = 9.2 \times 10^4$ M$^{-1}$ and $K_{E\text{-AzoIm}} = 3.5 \times 10^4$ M$^{-1}$) under ambient conditions (ESI, Fig. S4 and S5†). When *E*-**3** isomerises to *Z*-**3** under UV irradiation at 360 nm, *Z*-**3** was preferentially included inside CB[8] (Fig. 1c). From the NMR spectra (ESI, Fig. S1f and S2f†), sharp peaks corresponding to the protons of **1** and **2** were shifted downfield while the broad peaks of CB[8]·*Z*-**3** were shifted upfield, which strongly suggested the exclusion of **1** and **2** from the host molecule after UV irradiation. Proton peaks of uncomplexed *E*-**3** are also observed in Fig. S1d, S1f and S2f† in the presence of CB[8] on account of incomplete photoisomerisation of *E*-**3** to its *cis* conformation in the UV region. UV-Vis spectra on the complexation–decomplexation mechanism of CB[8], methyl viologen, naphthyl and AzoIm molecules before and after photoirradiation were in agreement with the NMR studies (ESI, Fig. S3†).

This observation was also supported by ITC titration of the *Z*-**3** enriched solution (at *E* : *Z* ratio of 20 : 80) into CB[8] whose binding constant ($1.2 \times 10^6$ M$^{-1}$, ESI, Fig. S6†) was higher than that of **1** ($8.5 \times 10^5$ M$^{-1}$).[20] For comparison, the binding constant for preformed CB[8]·*Z*-**3** and **1** was too small to be measured by ITC. On account of the stronger interaction between the positively-charged moiety and CB[8] portal, the cationic *cis*-azobenzene displaces other guests including viologen derivatives and fully occupies CB[8] in a 1 : 1 manner.[19,21] This was clearly shown by the X-ray crystal structure of the CB[8] *Z*-**3** complex in which the *cis*-azobenzene guest resides inside the macrocyclic cavity and the charged imidazolium group lies at one of the ureido carbonyl portals of CB[8] (Fig. 2).

### 2.2 Photo-induced rheological modifications of PRFs

On account of the findings from the NMR analysis of the model compounds, the guest molecules were introduced into
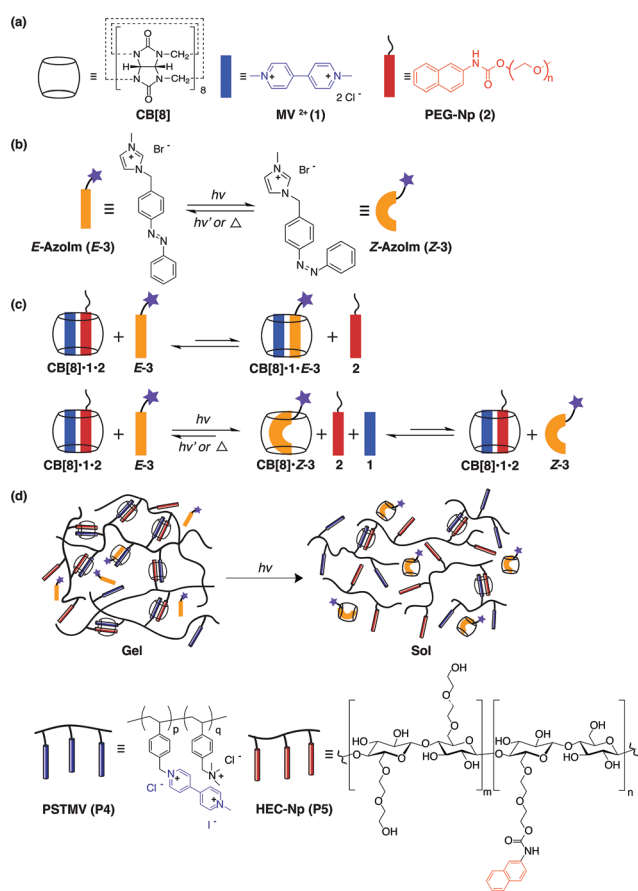


**Fig. 1** Structures of cucurbitl[8]uril (CB[8]), guest molecules **1** and **2**, which are model compounds for the viologen and naphthyl units on polymers **P4** and **P5** (a); photoisomerisation of azobenzene imidazolium (b); the equilibrium state of CB[8]·**1**·**2** in the presence of **3** before and after UV irradiation (c) and the scheme of photo-induced gel-to-sol transition of the HEC polymer network formed by CB[8]·**P4**·**P5** complexation in the presence of the competitive guest, *E*-**3**, under UV irradiation (d).
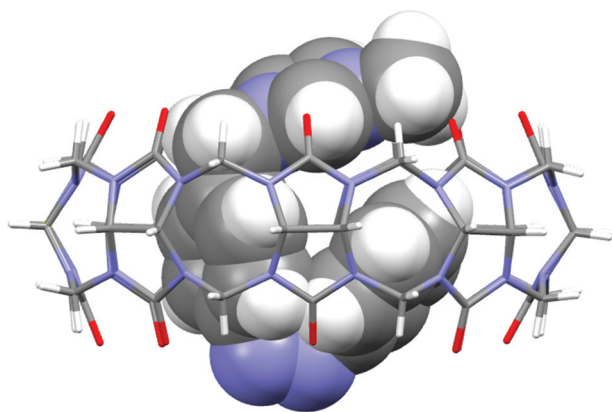
**Fig. 2** Side view of the X-ray crystal structure of CB[8]·Z-**3**. C, grey; N, blue; O, red; H, white.



**Fig. 3** Storage (*G′*) and loss (*G″*) moduli from dynamic rheology at 1% strain (a) and steady-shear rheology (b) of 0.75 wt% HEC polymer networks containing 0.5 mol eq. *E*-**3** before and after UV irradiation (360 nm, 4.8 mW cm$^{-2}$, 5 min, 20 °C).

selected polymers (see the Experimental section in the ESI†) in order to construct a polymer network. An aqueous, transparent and rigid polymer network is easily achieved by using low concentrations (≤0.75 wt%) of high-molecular-weight polymers, with CB[8] as the macrocyclic host in forming a heteroternary 1 : 1 : 1 binding motif. This viscoelastic polymer network exhibits high viscosity at 0.5 wt% **P5** (5 mol% Np), 0.15 wt% **P4** (10 mol% MV) and 0.1 wt% CB[8]. The 3D polymer network remained unperturbed upon the addition of light-responsive AzoIm (*E*-**3**), as supported by the inverted vial tests (Fig. 3b(ii)). On the other hand, the presence of AzoIm endows the supramolecular system with photosensitivity.

In principle, the photoisomerisation of *E*-AzoIm to *Z*-AzoIm under UV light disrupts the host–guest complexation, leading to a viscosity drop in the fluid (Fig. 1d). When the sample was exposed to 5 min UV irradiation (360 nm, 4.8 mW cm$^{-2}$, 20 °C), a remarkable gel-to-sol transition was observed in an inverted vial test illustrated in Fig. 3b (iii). To further quantify the light-induced rheological changes of the polymer network, dynamic rheology was studied by comparing its storage (*G′*) and loss (*G″*) moduli as a function of frequency. Before photoirradiation, an initial 20 Pa decrease in *G′* was observed when 0.5 mol eq. *E*-**3** was added to the HEC polymer network (ESI, Fig. S7a and S8†) corresponding to *E*-**3** competing with **P5** for the CB[8]·**P4** complex. The *E*-**3** concentration introduced to the polymer solution was only 50% of the Np moieties on **P5**. As shown in Fig. 3, the sample shows a purely viscoelastic, non-Newtonian response in the presence of *E*-**3** prior to UV irradiation. The gel network remained intact on account of the stable CB[8]·**P4**·**P5** heteroternary complexation.

Upon UV irradiation (360 nm, 4.8 mW cm$^{-2}$, 5 min, 20 °C), *E*-**3** underwent a conformation change to its *cis* geometry and formed a binary complex CB[8]·*Z*-**3**, accelerating the dissociation of the CB[8]·**P4**·**P5** network (Fig. 1d). A gel-to-sol transition was confirmed in Fig. 3a, where *G″* > *G′* as a function of frequency. From the steady-shear rheology (viscosity *vs.* shear stress), the zero-shear viscosity of the HEC sample decreased by more than two orders of magnitude at low shear rates and a
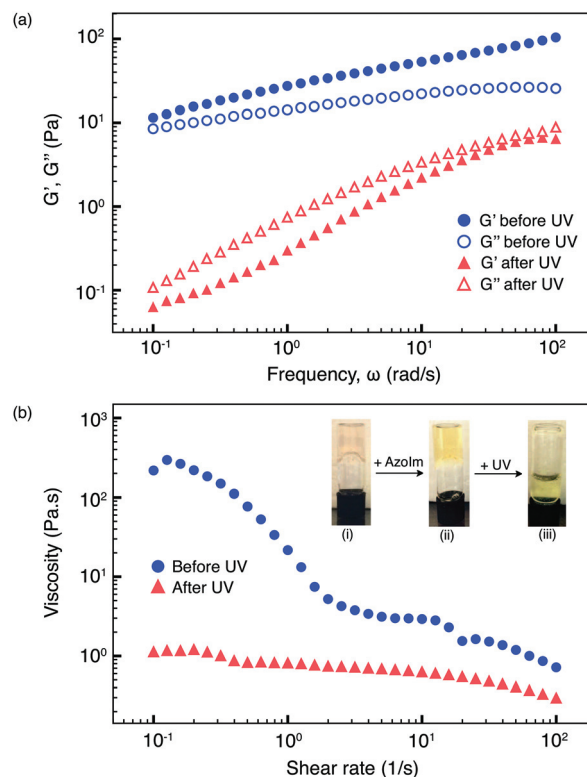
Newtonian-like fluid was obtained after UV irradiation (Fig. 3b). A similar or lesser extent of viscosity reduction under UV light has also been previously reported for other systems, but at much higher contents of the polymer or surfactant.[5,11,22] Therefore, the PRF based on the CB[8]-mediated polymer network achieved more significant viscosity reduction under UV irradiation from the perspective of the solid content used. Moreover, the transparent HEC-based PRF possesses a low optical density in the visible light region, which is beneficial for some specific optical applications. There were no obvious changes in the rheological properties of HEC samples alone as both the moduli are independent of frequency and displayed a non-Newtonian behaviour (ESI, Fig. S7†). This observation indicates that the rheological changes in the polymer network mainly correspond to the degree of crosslinking stemming from the CB[8]–guest interactions, therefore, eliminating the effect caused by the degradation of the polymer backbone. Photo-induced rheological modification on the PRF is based on the highly stable complexation of cationic *Z*-**3** and CB[8], displacing **P4** and **P5** guests from the macrocyclic host cavities. This results in the disassembly of the 3D network formed by CB[8]·**P4**·**P5**, as supported by the NMR spectra of the model compounds (ESI, Fig. S1 and S2†). Rearrangement of the molecular packing and reduced entanglement of the polymer chains from host–guest complexation–decomplexation produce a low-viscosity Newtonian-like fluid with *G″* > *G′*.

In contrast, a neutral azobenzene molecule does not behave in a similar manner with CB[8] as the cationic azobenzene derivatives under UV irradiation.[18,19] In a heteroternary complex, the $Z$ isomer of a neutral azobenzene is displaced from the cavity of CB[8], leaving the CB[8]·**1** binary complex intact.[18] To demonstrate this, we added neutral $E$-AzoTEG to the supramolecular polymer network by following the same protocol as a control. No significant changes in the viscosity and viscoelastic moduli occurred to the HEC samples containing $E$-AzoTEG after UV irradiation (ESI, Fig. S9†). This observation demonstrates specific yet robust CB[8]-assisted complexation; hence, a careful selection of competitive light-responsive guest molecules is essential to achieve the desired control over rheological properties.

We have already shown that appreciable macroscopic changes and rheological modifications can be induced in the supramolecular polymer network from direct photoisomerisation of $E$-**3** in the UV region. The evolution of the rheological properties as a function of UV irradiation time and azobenzene concentration was also investigated (ESI, Fig. S10–S12†). UV exposure of 5 min (360 nm, 4.8 mW cm$^{-2}$, 20 °C) was the shortest time required to reduce the zero-shear viscosity to 1 Pa·s, resulting in a Newtonian-like fluid (ESI, Fig. S10a†). We also demonstrated that this HEC-based PRF only required a low concentration of a photoresponsive moiety (0.5 mol eq.) to obtain a low-viscosity fluid (ESI, Fig. S10b†). Further reduction in the viscoelastic components was observed corresponding to longer UV exposure and increasing azobenzene concentration, and this was evident by the gradual shift of the $G'$, $G''$ crossover point towards higher frequencies (ESI, Fig. S11 and S12†).

### 2.3 Real-time photo-rheology measurements

Real-time photo-rheology measurements (320–390 nm, 28 mW cm$^{-2}$, 20 °C) in Fig. 4 further confirm the fast gel–sol switch in only 40 s, with a drastic drop in the complex viscosity and its moduli ($G'' > G'$). We also performed repetitive photo-rheological measurements under alternate UV and visible light
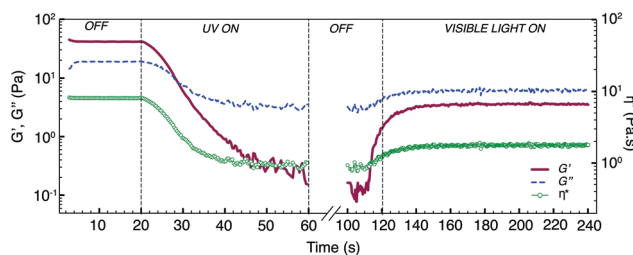
**Fig. 5** Real-time cyclic photoswitching of 0.75 wt% HEC sample with 0.5 mol eq. of $E$-**3** at 20 °C under alternate UV-visible light irradiation. During UV irradiation (320–390 nm, 40 s), the $G'$ (green circles) and complex viscosity, $\eta^*$ (red squares) decreased immediately. $G'$ and $\eta^*$ increased but did not regain their initial values during visible light irradiation (400–500 nm, 1200 s).

irradiation on the HEC-samples containing $E$-**3** (Fig. 5). After the first cycle of visible light irradiation (400–500 nm, 20 min, 20 °C), $G'$ increased slightly from 0.2 Pa to 3 Pa. Nonetheless, the initial moduli and complex viscosity of the fluids were not restored in subsequent visible light irradiation. The changes in $G'$ and complex viscosity of the matrix were consistent throughout several cycles of successive UV-visible light irradiation, implying that the *trans–cis* photoisomerisation of azobenzene had reached a photostationary equilibrium and could be repeated many times without decomposition of the components. As controls, the moduli and complex viscosity of HEC containing the $E$-AzoTEG sample and the HEC sample alone remained constant throughout the photoswitching (ESI, Fig. S13†).

Controlled reversible photochemical processes of azobenzene derivatives have been well documented.[23–28] However, the recovery of $Z$–$E$ azobenzene by photoirradiation has been reported to be incomplete or limited in aqueous solution when azobenzene is encapsulated in a host molecule.[29,30] In our case, the photoswitchability of azobenzene derivatives is greatly influenced by its CB[8]·**1** complexation. Subsequent visible light ($\lambda > 420$ nm) irradiation on $Z$-azobenzene alone results in 90% recovery of the *trans* isomer. Nevertheless, $Z$-**3** alone could be recovered completely to its *trans* state upon heating at 70 °C for 24 h on account of $Z$-to-$E$ thermoisomerisation (ESI, Fig. S14†). The photoisomerisation of $E$-**3** within the heteroternary complex CB[8]·**1**·$E$-**3** to its $Z$ conformation and *vice versa* was much slower than that of uncomplexed $E$-**3**. The predominant CB[8]·$Z$-**3** species remaining after visible light irradiation was attributed to the enhanced stability of the complex in the solution, which was in agreement with our previous findings with a different positively-charged azobenzene derivative.[19] While $G'$ and $G''$ of the polymer network increased upon *in situ* visible light irradiation or heating, their initial

**Fig. 4** Real-time photo-rheology of the 0.75 wt% HEC sample with 0.5 mol eq. of $E$-**3** at 20 °C. Upon UV irradiation (320–390 nm, 40 s), the $G'$ (solid red line) and $G''$ (dotted blue line) decreased immediately. Complex viscosity, $\eta^*$ (green circles) of the sample also dropped after UV irradiation. The $G'$ and $G''$ increased but did not regain their initial values during visible light irradiation (400–500 nm, 1200 s). OFF refers to no photoirradiation, ON refers to UV-visible light irradiation. A change of filter between 320–390 nm and 400–500 nm took place in between photoirradiation.
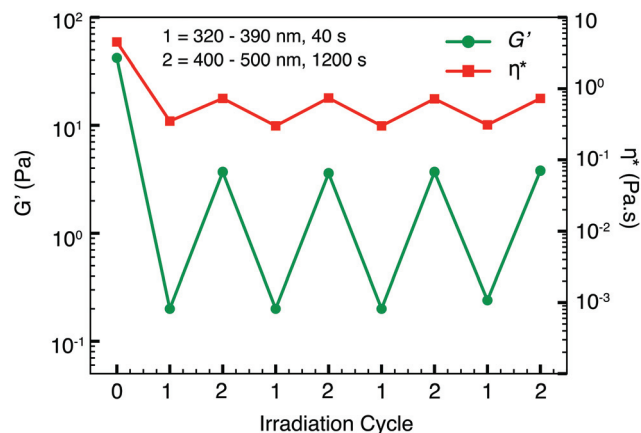
moduli and viscosity were not completely regained (ESI, Fig. S15†). Nevertheless, the low-viscosity solution can be converted back to the gel state by adding excess CB[8] into the polymer matrix (ESI, Fig. S16†). Similar non-reversible viscosity recovery using photoirradiation at different wavelengths is also reported in micellar PRFs. The reversibility of such systems could be achieved by altering their mixture composition and pH.[5,13]

### 2.4 Self-healing properties of PRF

On the basis of extremely fast association kinetics of the CB[8] ternary complex formation,[31] this supramolecular polymer network could recover its mechanical properties rapidly after deformation.[16,17] Step-strain measurements were performed to investigate the recovery properties of CB[8]·$P4$·$P5$ networks in the presence of $E$-3 following rupture at high strain. A high-magnitude strain ($\varepsilon$ = 1000%) was applied to destroy the 3D structure, followed by a low magnitude strain ($\varepsilon$ = 0.05%) to monitor the recovery rate of the bulk material properties. The rapid self-healing nature of HEC-based PRFs is clearly unaffected by the presence of the competing guest $E$-3 and its extent of recovery remained stable over five cycles of deformation and reassembly (ESI, Fig. S17†). Moreover, these supramolecular networks have been previously reported to be thermoresponsive,[17] in which their viscoelastic components decreased with heat and gradually rose back to their initial moduli without significant changes after the cooling process (ESI, Fig. S18†). The reversible nature of CB[8] ternary complexation highlights the flexibility of our system as a photothinning PRF material.

## 3. Conclusion

In conclusion, we have successfully established a CB[8]-mediated supramolecular polymer network as an aqueous PRF with light-tunable rheological properties at extremely low polymer and chromophore concentrations. This polymer network has a low optical density and consists of viologen- and naphthyl-bearing hydrophilic polymers ($P4$, $P5$) dynamically crosslinked by CB[8] in the presence of photoisomerisable azobenzene imidazolium ($E$-3). The light-responsiveness of $E$-3 allows the remotely photocontrolled complexation–decomplexation process of CB[8] ternary complexes, leading to changes in mechanical and flow properties of the polymer network. The remarkable stabilisation of CB[8]·$Z$-3 disrupted the inter-chain physical crosslinks formed *via* CB[8]·$P4$·$P5$, resulting in the overall decrease of polymer entanglements in the polymer network.

A rapid decrease in the zero-shear viscosity and viscoelastic moduli by 2–3 orders of magnitude could be readily induced in this shear-thinning fluid by UV irradiation for a few minutes. Moreover, a facile spatiotemporal control of PRF rheological properties can also be accomplished by varying the duration of photoirradiation and concentration of the small molecule cationic azobenzene moiety. The self-healing behaviour of this cellulose-based PRF in the presence of the azobenzene photoswitch, bestowed by the dynamic CB[8]–guest interactions, could thus be valuable for use in microscale flow-control devices and sensors.

## Acknowledgements

## References

1 R. Stanway, *Mater. Sci. Technol.*, 2004, **20**, 931–939.
2 K. Tsuchiya, Y. Orihara, Y. Kondo, N. Yoshino, T. Ohkubo, H. Sakai and M. Abe, *J. Am. Chem. Soc.*, 2004, **126**, 12282–12283.
3 J. de Vicente, D. J. Klingenberg and R. Hidalgo-Alvarez, *Soft Matter*, 2011, **7**, 3701–3710.
4 Z. Chu, C. A. Dreiss and Y. Feng, *Chem. Soc. Rev.*, 2013, **42**, 7174–7203.
5 A. M. Ketner, R. Kumar, T. S. Davies, P. W. Elder and S. R. Raghavan, *J. Am. Chem. Soc.*, 2007, **129**, 1553–1559.
6 I. B. Jang, H. B. Kim, J. Y. Lee, J. L. You, H. J. Choi and M. S. Jhon, *J. Appl. Phys.*, 2005, **97**, 10Q912.
7 L. Peng, M. You, Q. Yuan, C. Wu, D. Han, Y. Chen, Z. Zhong, J. Xue and W. Tan, *J. Am. Chem. Soc.*, 2012, **134**, 12302–12307.
8 J. Zheng, Y. Nie, S. Yang, Y. Xiao, J. Li, Y. Li and R. Yang, *Anal. Chem.*, 2014, **86**, 10208–10214.
9 V. Gatterdam, R. Ramadass, T. Stoess, M. A. H. Fichte, J. Wachtveitl, A. Heckel and R. Tampé, *Angew. Chem., Int. Ed.*, 2014, **53**, 5680–5684.
10 R. Kumar, A. M. Ketner and S. R. Raghavan, *Langmuir*, 2010, **26**, 5405–5411.
11 H. Y. Lee, K. K. Diehn, K. Sun, T. Chen and S. R. Raghavan, *J. Am. Chem. Soc.*, 2011, **133**, 8461–8463.
12 H. Shi, W. Ge, H. Oh, S. M. Pattison, J. T. Huggins, Y. Talmon, D. J. Hart, S. R. Raghavan and J. L. Zakin, *Langmuir*, 2013, **29**, 102–109.
13 K. Sun, R. Kumar, D. E. Falvey and S. R. Raghavan, *J. Am. Chem. Soc.*, 2009, **131**, 7135–7141.
14 H. Oh, A. M. Ketner, R. Heymann, E. Kesselman, D. Danino, D. E. Falvey and S. R. Raghavan, *Soft Matter*, 2013, **9**, 5025–5033.
15 J. E. Koskela, J. Vapaavuori, R. H. A. Ras and A. Priimagi, *ACS Macro Lett.*, 2014, **3**, 1196–1200.
16 E. A. Appel, F. Biedermann, U. Rauwald, S. T. Jones, J. M. Zayed and O. A. Scherman, *J. Am. Chem. Soc.*, 2010, **132**, 14251–14260.

17 E. A. Appel, X. J. Loh, S. T. Jones, F. Biedermann, C. A. Dreiss and O. A. Scherman, *J. Am. Chem. Soc.*, 2012, **134**, 11767–11773.

18 F. Tian, D. Jiao, F. Biedermann and O. A. Scherman, *Nat. Commun.*, 2012, **3**, 1207.

19 J. del Barrio, P. N. Horton, D. Lairez, G. O. Lloyd, C. Toprakcioglu and O. A. Scherman, *J. Am. Chem. Soc.*, 2013, **135**, 11760–11763.

20 M. E. Bush, N. D. Bouley and A. R. Urbach, *J. Am. Chem. Soc.*, 2005, **127**, 14511–14517.

21 H.-B. Cheng, Y.-M. Zhang, C. Xu and Y. Liu, *Sci. Rep.*, 2014, **4**, 4210.

22 I. Tomatsu, A. Hashidzume and A. Harada, *J. Am. Chem. Soc.*, 2006, **128**, 2226–2227.

23 Y. Wang, N. Ma, Z. Wang and X. Zhang, *Angew. Chem., Int. Ed.*, 2007, **119**, 2881–2884.

24 A. S. Kumar, T. Ye, T. Takami, B.-C. Yu, A. K. Flatt, J. M. Tour and P. S. Weiss, *Nano Lett.*, 2008, **8**, 1644–1648.

25 Y. Zhou, D. Wang, S. Huang, G. Auernhammer, Y. He, H.-J. Butt and S. Wu, *Chem. Commun.*, 2015, **51**, 2725–2727.

26 C. Stoffelen, J. Voskuhl, P. Jonkheijm and J. Huskens, *Angew. Chem., Int. Ed.*, 2014, **53**, 3400–3404.

27 G. Yu, C. Han, Z. Zhang, J. Chen, X. Yan, B. Zheng, S. Liu and F. Huang, *J. Am. Chem. Soc.*, 2012, **134**, 8711–8717.

28 M. Liu, X. Yan, M. Hu, X. Chen, M. Zhang, B. Zheng, X. Hu, S. Shao and F. Huang, *Org. Lett.*, 2010, **12**, 2558–2561.

29 X. Chi, X. Ji, D. Xia and F. Huang, *J. Am. Chem. Soc.*, 2015, **137**, 1440–1443.

30 D. Xia, G. Yu, J. Li and F. Huang, *Chem. Commun.*, 2014, **50**, 3606–3608.

31 E. A. Appel, R. A. Forster, A. Koutsioubas, C. Toprakcioglu and O. A. Scherman, *Angew. Chem., Int. Ed.*, 2014, **53**, 10038–10043.